Spectral characteristics of water vapor in UV spectral region

M.M. Makogon

Institute of Atmospheric Optics,
Siberian Branch of the Russian Academy of Sciences, Tomsk

Received August 30, 2001

The results on the water vapor absorption and fluorescence spectra in the near-UV spectral region are analytically reviewed.

Introduction

Water vapor absorption in the region of rotational-vibrational transitions (visible and infrared spectral regions) is being studied rather actively, what is reflected in a number of specialized publications.[1] The measurements of water vapor absorption in the region of electronic transitions[2,3] for many years did not touch the region beyond 106–198 nm (photographic measurements of the water vapor absorption coefficients[4] in the region of 145–185 nm are low-informative). In the experiments on electron scattering, wide bands (the so-called 4.5-eV bands, for brief analysis see Ref. 5) are observed. However it is believed[6] that these bands are not related to photoprocesses in H_2O vapor. This state of experimental research was "supported" by the results of theoretical quantum-chemistry calculations demonstrating the absence of electronic states with the energy of the vertical transition less than 6.2 eV ≈ 49800 cm^{-1}.

In 1980 (Ref. 7) when studying Raman scattering of light by minor atmospheric constituents under the exposure to near-UV laser radiation (second harmonic of ruby laser and fourth harmonic of Nd:YAG laser) in the region up to 3000 cm^{-1} from the exciting line, re-emission was found, and the value of this re-emission correlated with the humidity of the atmosphere and the state of precipitation. Direct measurements in artificial mixtures[8] showed that earlier detected signals were caused by water vapor. Further experimental studies by use of different laser spectroscopy methods gave vast information on the absorption and fluorescence of water vapor in the region of 213–425 nm, which is being reviewed in this paper.

The interest to the studies of spectral characteristics of water vapor in the near-UV region is also motivated by the following circumstances.

1. Extinction of solar radiation in the near-UV spectral region is mostly determined by ozone, and all calculations of the radiative fluxes in this spectral region use approximations of the transmission function based on the ozone absorption spectrum. However, already in 1950 as early (Ref. 9) it was stated that water vapor absorption might be a significant factor in extinction of solar radiation; in fact, these papers, stimulated the measurements conducted in Ref. 2.

2. Almost any of optical ozonometers (see, for example, Ref. 10) measuring the total ozone content in the atmosphere is operated following the common scheme – they measure extinction of solar radiation in selected spectral ranges. Additional extinction due to water vapor is ignored in this case and the results are thus overestimated. The overestimation can be found from the H_2O absorption spectrum. Although the corrections to the ozone concentrations determined in such a way are small (absorption by water vapor is markedly lower than that by the ozone), they may prove significant, because the ozone determines many atmospheric chemical reactions.

3. The near-UV region is now used for sensing various chemical compounds by lidars using the method of laser-induced fluorescence. For correct separation of spectra and determination of the concentrations of individual gases, it is necessary to know accurately the atmospheric transmittance.[11] Simple models of extinction of UV radiation[12] accounting for contributions coming from aerosol, molecular scattering, and absorption by oxygen and ozone do not provide for the desirable accuracy. Moreover, the measurement error in the spectral atmospheric transmittance in the UV region now does not exceed 1% nearby 310 nm and 0.2% nearby 400 nm (Ref. 13), whereas the contribution of H_2O to the extinction of UV radiation is about 3% of the total extinction coefficient at the wavelength of 310 nm (Ref. 14). Therefore, it is necessary to take into account the effect of atmospheric water vapor.

4. Finally, the increasing capabilities of calculating higher and higher rotational-vibrational states[15] allow us to look forward at the direct comparison of experimentally measured and calculated near-UV absorption spectra in the nearest future.

Experimental data

Absorption spectra

The water vapor absorption spectrum in the region from 106 to 186 nm was obtained in Ref. 2 and Ref. 3 (185–198 nm) and is depicted in Fig. 1. The length of a single-pass cell was 4.7 and 10 cm, and the water vapor pressure was 0.08 to 8 and 20 mm Hg column, respectively, in Refs. 2 and 3. The resolution of the

0235-6880/01/09 696-11 $02.00

monochromator in Ref. 2 was about 0.1 nm. Water vapor was produced from distilled water additionally rectified[2] by distillation at 0°C in a vacuum rectification system; mass-spectrometric analysis showed that the total pollution was within 0.05%. To obtain stable results, the cell upon being filled was held for about 1 h until the pressure reached the equilibrium.[2]

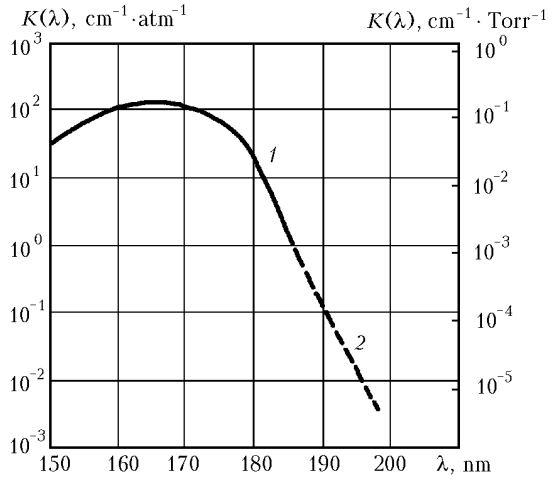

Fig. 1. Water vapor absorption spectrum in the region from 150 to 198 nm: data from Refs. 2 (*1*) and 3 (*2*).

Measurements in the longer-wave spectral region were conducted with the optical path length of 104 (Ref. 16), 64 (Ref. 17), 440 (Ref. 18), and up to 1320 m (Ref. 19). Toward this end, multipass gas cells with the separation of 2.2, 2, and 10 m between mirrors were filled with water vapor. The sources of radiation were quartz-halogen bulb,[17] dye laser,[16] Nd:YAG laser,[19,18] and neodymium-doped glass laser,[19] whose frequency was converted into the UV region through harmonic generation. The spectral resolution in Ref. 17 was roughly 1, 0.3, and 0.1 nm in the ranges of 265–280, 280–300, and 300–360 nm. The spectral width of laser radiation did not exceed 0.03 nm (Ref. 16) and 0.14 pm (Ref. 19); the pulse-to-pulse step of frequency tuning was 0.14–0.35 pm (Ref. 19).

The measured absorption spectra are depicted in Fig. 2. In a specialized methodical experiments,[16] it was found that the dependence of the H_2O absorption coefficient (at the wavelength of 277.8 nm) reduced to the unit pressure ($\tilde{K} = K/P_{H_2O}$) on the H_2O vapor pressure keeps almost unchanged up to $P_{H_2O} \le 12$ Torr (Fig. 2*b*), therefore the absorption spectra were recorded in Ref. 16 at the pure water vapor pressure of 10 Torr.

In Ref. 19, the object of study was atmospheric air at the total pressure of 750–760 Torr and the partial pressure of water vapor of 9.9 or 10 Torr (Fig. 2*c*). The measured absorption cross section for the YAG laser radiation turned out to be equal to $(4.9 \pm 0.1)\cdot 10^{-23}$ cm^2 [$K(\lambda) = (1.74 \pm 0.03)\cdot 10^{-6}$ cm$^{-1}\cdot$Torr^{-1}], the mean value of the absorption coefficient in the interval of 263–268 nm for a tunable neodymium-doped glass laser was $(1.83 \pm 0.12)\cdot 10^{-5}$ cm^{-1}.

The absorption coefficient determined in Ref. 18 at the wavelength of 266 nm was $8\cdot 10^{-7}$ cm$^{-1}\cdot$Torr^{-1}.

The water vapor absorption spectrum was measured in the process of detailed studies of liquid water absorption at $\lambda = 180 - 500$ nm (Ref. 20). It was concluded that water vapor absorption coefficient at different temperature is proportional to the concentration of vapor molecules, and the spectral dependence is identical to that for the liquid water (this does not coincide with Refs. 21 and 22, see below). The analytical dependence of the exponential absorption coefficient of water vapor under standard conditions (T = 273 K, pressure of 760 Torr) corresponding to the experimental results has the following form:

$$\varepsilon = 92 \exp\left[16.9\,(\lambda^{-1} - \lambda_0^{-1})\right] \qquad (1)$$

(ε, in m^{-1}; λ and λ_0, μm; $\lambda_0 = 0.186$ μm).

The UV water vapor absorption spectra at a high temperature (1000–3700 K) were measured in a shock-wave tube[23] (Fig. 3).

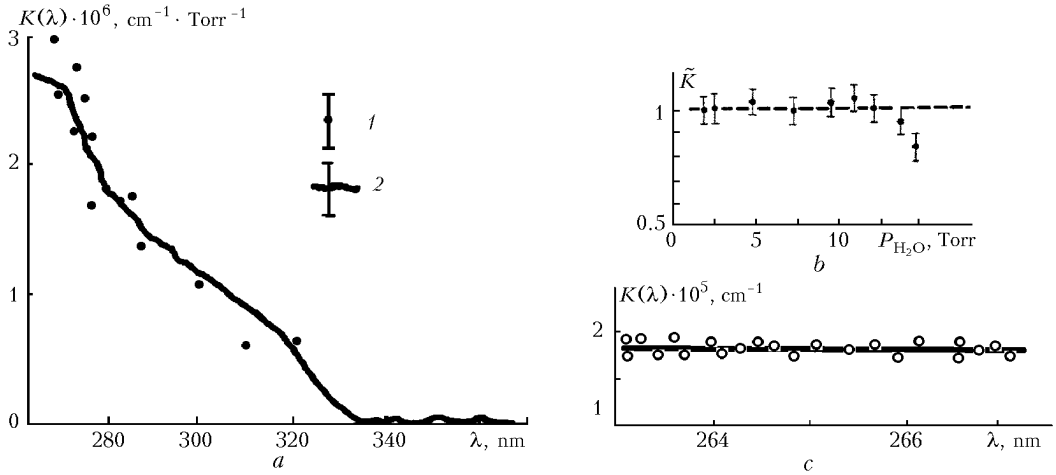

Fig. 2. Spectral water vapor absorption coefficient in the region of 260–370 nm for pure water vapor (*a*): data from Refs. 16 (*1*) and 17 (*2*); dependence of the normalized absorption coefficient on the total water vapor pressure, Ref. 16 (*b*); dependence of the air absorption coefficient, Ref. 19 (*c*).

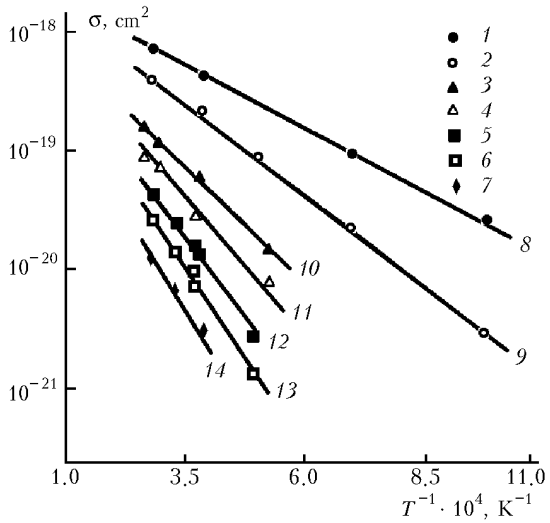

Fig. 3. The absorption cross section of H_2O molecules for UV radiation: experiment (*1–7*) and calculation by Eq. (2) (*8–14*); λ = 190 (*1*, *8*), 196.4 (*2*, *9*), 210 (*3*, *10*), 216.4 (*4*, *11*), 225 (*5*, *12*), 231.4 (*6*, *13*), and 241.4 nm (*7*, *14*).

In the studied temperature and wavelength ranges, the H_2O absorption cross section is well described by the equation

$$\sigma(\lambda, T) = \sigma_0(\lambda) \exp(-\theta/T), \qquad (2)$$

where $\log[\sigma_0(\lambda)] = -15.598 - 0.0103 \cdot \lambda$ and $\theta = 33664 - 202.6 \cdot \lambda$ (here λ is in nm).

Photo-acoustic spectra

The water vapor absorption spectra were measured by the photo-acoustic method for the wavelengths of 266 nm (fourth harmonic of Nd:YAG laser[24]) and 255, 271, and 289 nm (harmonics and fundamental frequency of a copper-vapor laser[25]). Photo-acoustic receivers were calibrated against the absorption by a binary mixture of acetone at the wavelength of 266 nm (Ref. 24) and methane at the wavelength of 3392 nm (Ref. 25) with nitrogen. The object of study in Ref. 24 was distilled water.

The absorption coefficients of the binary mixture of water vapor with nitrogen determined by the standard method have the following values: $3.1 \cdot 10^{-7}$ cm^{-1}·Torr^{-1} (λ = 255 nm), $1.2 \cdot 10^{-7}$ cm^{-1} · Torr^{-1} (λ = 271 nm), and $2.0 \cdot 10^{-7}$ cm^{-1} · Torr^{-1} (λ = 289 nm) with the error of about 25%.

A large-volume optical cell and time-resolved measurements of signals allowed separation of signals connected with absorption by cell windows and the gas under study.[24] The value of a photo-acoustic response is linearly related to water vapor partial pressure (Fig. 4), and the coefficient of proportionality depended on the mixture composition. The absorption coefficient averaged over measurements in all mixtures (with air, nitrogen, and argon) was $(1.3 \pm 0.2) \cdot 10^{-7}$ cm^{-1} · Torr^{-1}.

The signal from windows is also related to the gas composition of the mixture in the cell. For non-absorbing gases (N_2, Ar, and H_2), the signal decreases 5–10 times as three to five laser pulses with the repetition rate of 1 Hz pass through the cell. If there is water vapor (pure or in a mixture with other gases) in the cell, the signal decreases only 2–3 times for 10 pulses, and it always is an order of magnitude or more higher than the useful signal from absorption in the gas. In Ref. 24, these facts are explained by adsorption of H_2O molecules on the surface of cell windows.

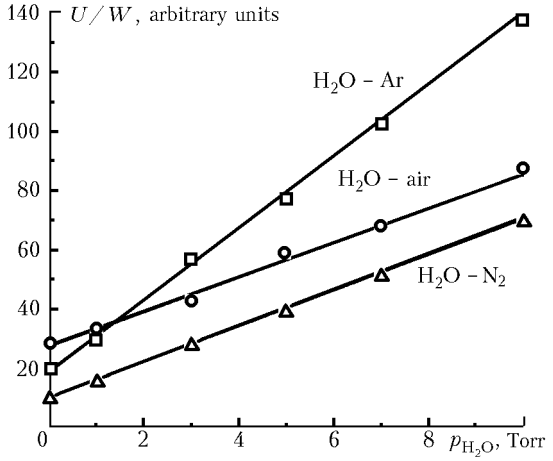

Fig. 4. The ratio of the amplitude of a photo-acoustic response U to the laser pulse energy W as a function of H_2O partial pressure in the cell at the total pressure of 100 Torr.

In Ref. 24, ionization of the gas mixture under the exposure to radiation with the wavelength of 266 nm in the pressure range of 10^{-3}–760 Torr was observed as well.

Fluorescence excitation spectra

The function of excitation of fluorescence in H_2O vapor under the exposure to radiation of KrF* laser, fourth harmonic of the Nd:YAG laser, XeCl* and N_2 lasers was studied in Ref. 26 and under the exposure to the second harmonic of the tunable dye laser – in Ref. 27.

The water vapor re-emission spectrum is independent of the exciting wavelength (Figs. 5*a–c*; the spectrum in Fig. 5*c* is distorted by the long-wave wing of the absorption filter used for suppression of scattered laser radiation; the dashed curves show the part of the spectrum corrected by subtraction of the absorption in filter). Figure 5*d* depicts the spectrum of long-wave part of the absorption band reconstructed from these data. This spectrum is obtained by normalizing the volumes under the surfaces of fluorescent signals in the coordinates λ, t, and I_{fl} to the laser pulse energy; the fluorescence signals were obtained in pure H_2O vapor. The value of K is the ratio of the scattered energy to the total energy of the laser pulse.

Fluorescence is excited with practically the same efficiency by a broadband and tunable (in the 30 Å

range, $\Delta\lambda$ = 3 Å) narrow-band radiation of a KrF* laser, as well as the narrow-band radiation of a Nd laser, thus indicating the continuum structure of the absorption band.

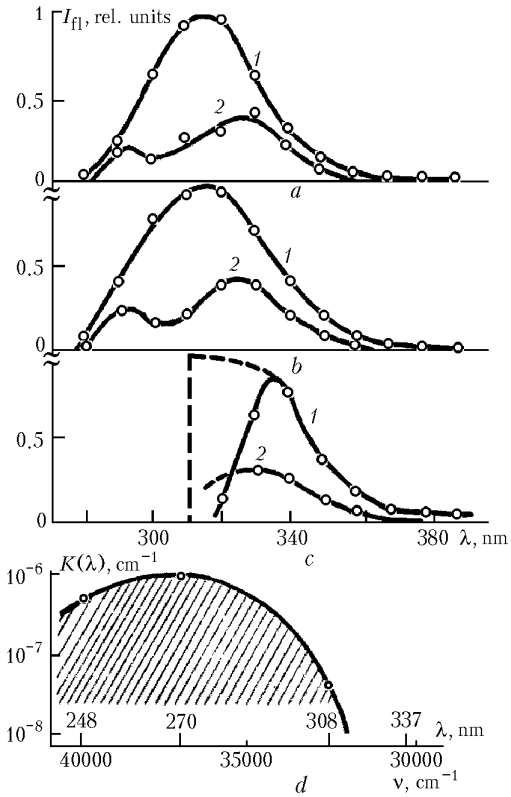

Fig. 5. Records of the water vapor fluorescence spectra (*a*–*c*) and its absorption band (*d*). Excitation by radiation at 248 (*a*), 270 (*b*), and 308 nm (*c*); signals correspond to time intervals of 0–50 (*1*) and 50–400 ns (*2*); H_2O vapor concentration of $4\cdot10^{17}$ cm^{-3}.

The excitation function was recorded in Ref. 27 with higher resolution (0.3 Å through the entire band and 0.03 Å in some its parts); it is depicted in Fig 6. The fine structure indicative of the discrete character of the spectrum was not revealed as well. Measurements were conducted in H_2O vapor; no data on pressure ware presented.

Water vapor fluorescence

In the first group of papers (Refs. 7, 8, 28–30, and 48), fluorescence and scattering spectra of atmospheric gases were studied in the Stokes range of detuning from the frequency of the exciting line (500–3500 cm^{-1}). The sources of radiation in Ref. 7 were solid-state lasers [second harmonic of the ruby laser (λ = 347 nm) and the fourth harmonic of the Nd:YAG garnet laser (λ = 266 nm)] and the measurements were conducted along open atmospheric paths, whereas in Refs. 8 and 28–30 the KrF* laser (λ = 248.5 nm) was used and the majority of data were obtained in measurements using cells.

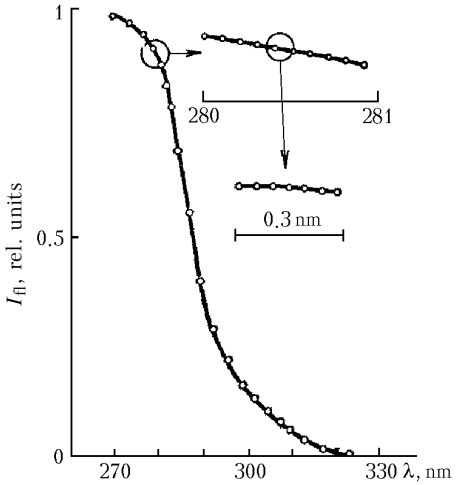

Fig. 6. Long-wave wing of the absorption band and its parts recorded with the resolution of 0.03 and 0.003 nm.

The response from the atmosphere depended on its state and the exciting wavelength.[7] The level of fluorescence was measured under different atmospheric conditions and during long time intervals, therefore the boundaries of the averaged values are given in Table 1.

Table 1. Level of atmospheric fluorescence in the region of 2000–3000 cm^{-1}, $\Delta\nu$ = 10 cm^{-1}

Wavelength, nm	Equivalent nitrogen concentration, ppm	
	Fog, rain, snow	No precipitation
347	300–500	50–200
266	20–100	20–50

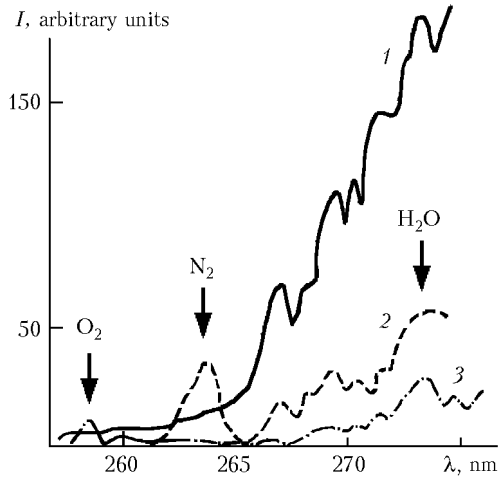

Fig. 7. Emission spectra of pure water vapor (*1*) and water vapor in a mixture with nitrogen (*2*) and oxygen (*3*) at excitation by radiation at 248.5 nm; arrows mark the positions of Raman lines; the water vapor pressure of 2.4 kPa, nitrogen pressure of 6.65 kPa, and oxygen pressure of 0.133 kPa.

In all papers, it was found that the intensity of the studied re-emission of the atmosphere increases with the distance from the exciting line and makes up 10^{-5} to 10^{-3} of the Raman signal from nitrogen in the 10-cm^{-1} band. Because of the shape of spectrum (Fig. 7) and the

presence of a large number of trapped photons (the signal was recorded with time resolution, the time-gate length varied from 50 to 800 ns), the observed spectrum was interpreted as a fluorescence spectrum.[28–30] It is also seen that at $\lambda \approx 266$ nm there exists a pronounced short-wave threshold of the fluorescence intensity.

Time-resolved analysis of the fluorescence response recorded within different time gates showed[28] that damping of fluorescence is roughly the same in different spectral intervals. The exponential character of fluorescence damping is illustrated in Fig. 8, which depicts the pressure dependences of the signals received in different time gates both for pure water vapor and for its mixtures with nitrogen and oxygen. The lifetime of a fluorescence responsible state in pure water vapor is (40 ± 3) ns and keeps unchanged within the measurement error at pressure variations from 0.4 to 2.4 kPa (Ref. 29). The cross section of fluorescence quenching by nitrogen and oxygen is about 10^{-17} and 10^{-14} cm^2, respectively[7] [the quenching rate constants are equal to $3 \cdot 10^{-12}$ and $1.4 \cdot 10^{-9}$ cm$^3 \cdot$ s^{-1} (Ref. 29)].

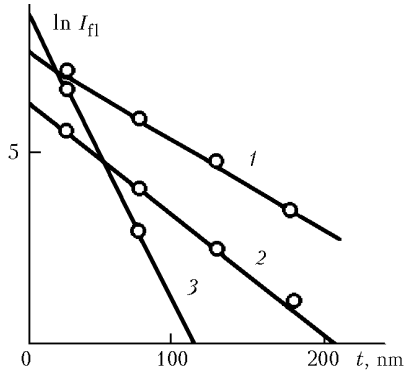

Fig. 8. Time dependence of the spectrally integral fluorescence intensity for pure water vapor (*1*) and its mixtures with nitrogen (*2*) and oxygen (*3*); the water vapor pressure of 2.4, nitrogen pressure of 6.65, and oxygen pressure of 0.133 kPa.

The spectrally integral fluorescence intensity in the pressure range from 0.8 to 2.4 kPa is quadratically depends on the H_2O concentration (Fig. 9). In Ref. 48, it was found that the intensity ratio of fluorescence to Raman scattering is proportional to the laser radiation power density (its variability range was not given). This points to the nonlinear character of the process of excitation of the observed fluorescence.

The measurements[29] have been conducted at focusing KrF* laser radiation with the maximum intensity reaching 5 GW/cm^2. In the area with the power density of 1–5 GW/cm^2, the spectrally integral fluorescence intensity weakly depended on the laser radiation intensity, thus being indicative of the saturation with the fluorescence excitation.

In Refs. 28, 29, and 48, two-photon dissociation of H_2O was assumed. However, if in Refs. 28 and 48 it was assumed that the observed fluorescence is caused by the OH radical produced in the process of dissociation, then Ref. 29 states that this does not agree with the full set of experimental data. It is assumed that fluorescence belongs to excited molecular oxygen produced in secondary photochemical processes following the dissociation of H_2O molecules.

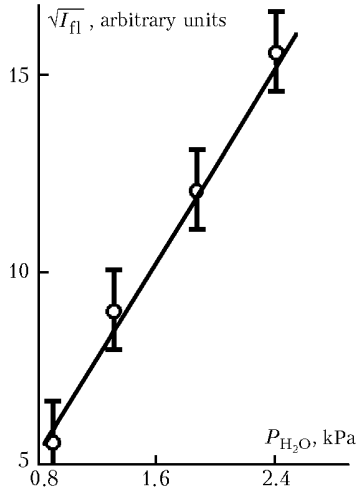

Fig. 9. Dependence of the spectrally integral fluorescence intensity on the water vapor pressure in the cell.

The atmospheric fluorescence spectrum in a wide region was recorded for the first time in Ref. 31 (Fig. 10). The study of various gas mixtures (air, water vapor, nitrogen, oxygen, argon, and helium in mixtures with each other) allowed the conclusion that either the H_2O molecule or its derivatives fluoresce.

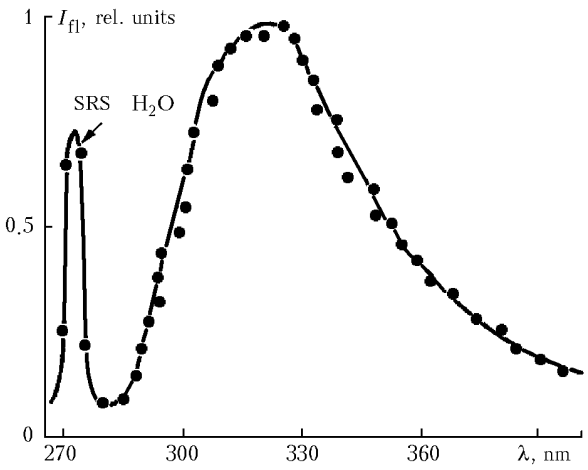

Fig. 10. Atmospheric fluorescence band induced by KrF* laser radiation.

It was found that in pure water vapor at the pressure of 0.01–15 Torr and in the mixture with inert gases the broad short-living (≤ 50 ns) spectrally continuous fluorescence band is complemented with at least two bands (one in the region of 315–360 nm and the other one in the region of 365 nm) with a significantly longer lifetime $\tau \approx 200$ ns (Fig. 11). Since the time between collisions is about 10^{-4} s under conditions of the experiment, the observed lifetimes are caused by intramolecular processes.

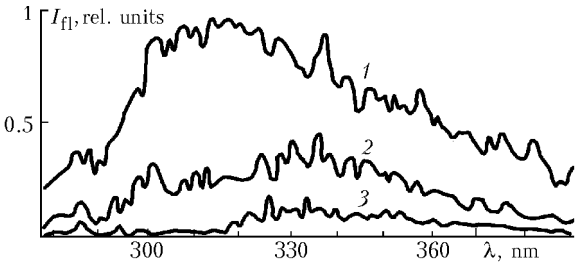

Fig. 11. H_2O fluorescence spectra successively recorded in three time intervals after termination of the exciting pulse: 0–50 (*1*), 50–100 (*2*), and 100–150 ns (*3*).

The fluorescence intensity practically linearly depends on the power density of the exciting radiation in the range $P_{exc} = 10^4 - 5 \cdot 10^5$ W/cm^2 (Fig. 12), thus indicating the single photon absorption process (processes connected with multiphoton absorption of radiation by water molecules were repeatedly observed[32]). Special measurements with laser radiation focused onto the cell[33] showed that at $P_{exc} > 10^8$ W/cm^2 the ruled fluorescence spectrum of the OH radical produced in the process of two-photon dissociation of water by the KrF* laser arises against the background of a broad fluorescence spectrum of water vapor; at lower P_{exc} this spectrum was not observed. Thus, in typical lidar experiments, OH is not responsible for the broadband fluorescence.

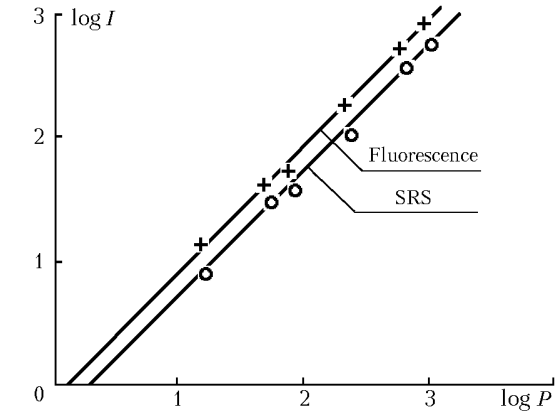

Fig. 12. Fluorescence and the SRS intensities of H_2O molecules as functions of power density of laser radiation.

The measurements of fluorescence intensity as a function of air and argon pressure (0–1 atm) at the saturated pressure of water vapor (about 15 Torr) showed that argon practically does not quench the fluorescence.[33] The quenching by air is rather significant and well described by the Stern–Volmer equation for the quenching factor

$$Q = 1/(1 + \sum_i q_i p_i) \qquad (3)$$

(p_i and q_i are the partial pressures and quenching factors of the gas components of the mixture) at the cross section $\sigma_{que} = 5 \cdot 10^{-16}$ cm^2.

Taking into account the single-photon process of excitation of the fluorescence observed under conditions that collisions can be neglected, as well as the large width of the emission spectrum of a KrF* laser (about 100 cm^{-1}), which can "cover" many H_2O absorption lines, Klimkin and Fedorishchev[33] believe that the observed fluorescence belongs to rotational-vibrational transitions in water molecule being in the ground state. The possibility of observing the fluorescence at excitation of rotational-vibrational transitions of the 000–103 water band by the ruby laser was analyzed earlier in Ref. 34.

Klimkin and Fedorishchev[33] reported that KrF* laser excites the characteristic fluorescence band in the mixtures containing D_2O as well.

In these papers, it was assumed that the H_2O molecule or its photochemical derivatives are responsible for the discussed fluorescence. However, the dimer $(H_2O)_2$ also may be a fluorescing object. This version was checked in Ref. 35 by measuring the fluorescence spectrum and cross section of water vapor at high temperature, because the concentration of dimers must decrease in this case.

The fluorescence was excited by the fourth harmonic of a Nd:YAG garnet laser (λ = 266 nm); the effect of scattered laser radiation on the recorded spectrum was excluded by a cut-off liquid benzene filter installed at the monochromator entrance. The measurements were conducted in air and pure vapor; the nitrogen Raman scattering line was used for absolute measurements of the fluorescence cross section. All available water samples were studied: distilled water, twice distilled water, medical water for injections, tap water from different sources, and the obtained results proved to be close.

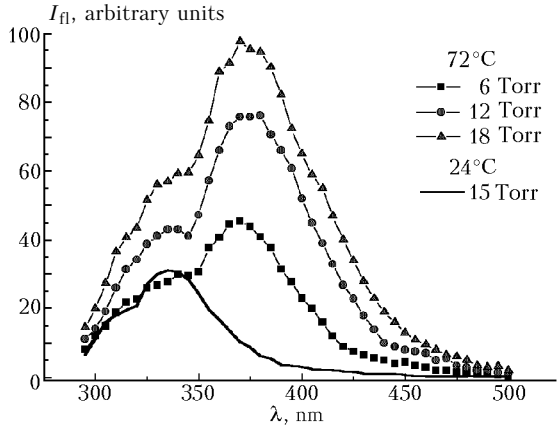

Fig. 13. Fluorescence spectrum of water vapor at the temperature of 24 and 72°C; excitation by radiation at 266 nm.

Figure 13 depicts the fluorescence spectrum of pure H_2O vapor at room and higher temperatures. As follows from the figure, the increase of temperature from 24 to 72°C causes sharp increase of the fluorescence in the region of 380 nm, and its cross section does not decrease, as it would be expected in the case of the dimer origin of this band, but even increases. The fluorescence was measured at different water vapor pressure, and this allowed the effect of collisions of

H_2O molecules on the fluorescence quenching to be estimated. The estimates agree well with those following from the Stern–Volmer equation. The obtained data are tabulated in Table 2.

Table 2. Parameters of water vapor fluorescence excited by radiation at 266 nm

Temperature, °C	Fluorescence cross section, 10^{-24} cm^2	Quenching factor q, Torr^{-1}	Quenching cross section σ_{que}, 10^{-15} cm^2
24	0.56	0.031	1.8
72	6.9	0.026	1.5

The fluorescence of water vapor was recently studied[36] in the case of excitation by the fifth harmonic of the Nd:YAG laser (wavelength of 212.8 nm, energy of 2 mJ, pulse duration of about 2 ns). The measurements were conducted using standard bistatic lidar optical arrangement. A 3-m cell was filled with water vapor (medical water for injections). The zone of overlapping of the exciting laser beam 1.5 cm in diameter and the telescope field of view was about 1 m and localized in the central part of the cell. The recording was performed in photon counting mode with time resolution.

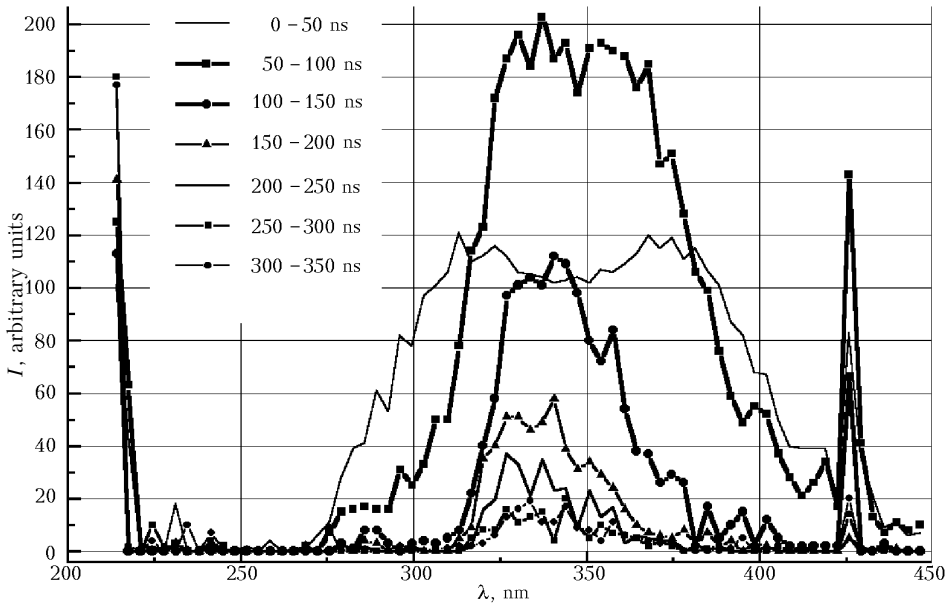

Fig. 14. Pure water vapor fluorescence spectra successively recorded in time intervals at excitation by radiation at 212.8 nm, the vapor pressure of 8 Torr. The emission peaks in the right-hand and left-hand parts are caused by the scattered laser radiation recorded in the first and second diffraction orders of the grating used.

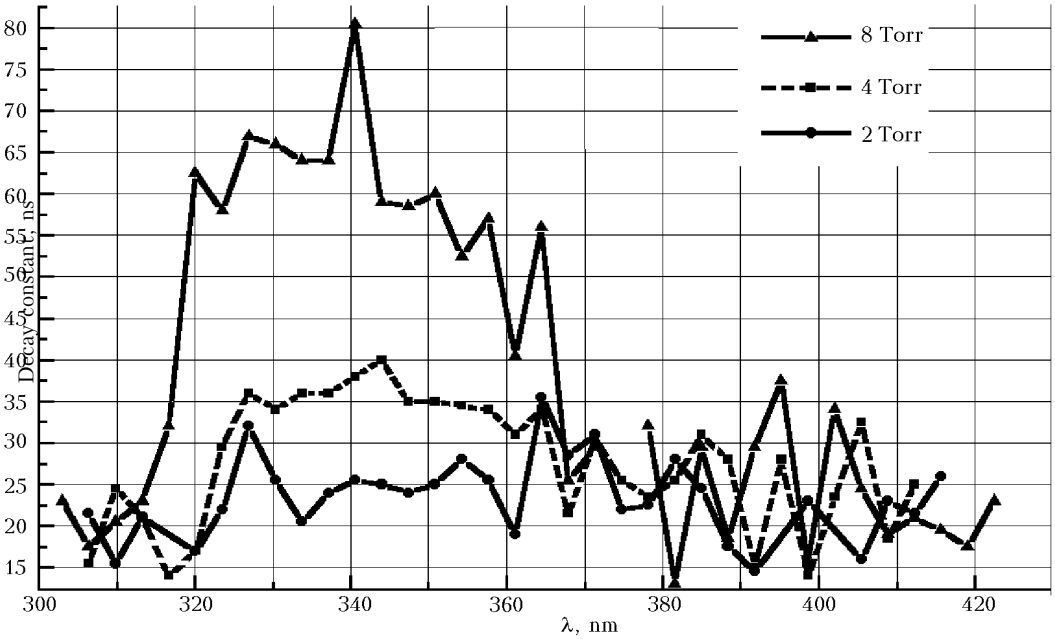

Fig. 15. Spectral dependence of the fluorescence decay constant of water vapor in the case of excitation by radiation at 212.8 nm.

The fluorescence is characteristic of the room temperature (Fig. 14), and its cross section is $2 \cdot 10^{-24}$ cm^2. The spectral-temporal behavior of the emission of pure water vapor allows us to separate three zones (Fig. 15) in the wavelength dependence of the fluorescence decay constant. At $\lambda < 315$ nm and $\lambda > 365$ nm the decay constant is equal to 15–25 and 15–35 ns, respectively, and independent of the vapor pressure. In the zone $315 < \lambda < 365$ nm, it increases approximately linearly with the vapor pressure. At the same time, the self-quenching cross section of the integral fluorescence is very large – $2.7 \cdot 10^{-13}$ cm^2.

Discussion

Studied samples

Preparation of samples is one of the crucial elements of the experimental research. Analysis of liquid water, especially in the UV region, is preceded by its purifying from organics, deionization, and double or triple distillation with the use of only medium portion in the following treatment (see Review 37). Thus, the most "pure" results were obtained when measuring absorption of liquid water in the UV spectral region.[38,39]

When studying water vapor, distilled water also was additionally prepared in some cases (distilled in a vacuum system[2] or passed through the repeated cycles: freezing (77 K) – evacuation (77 K) – melting (300 K) for degassing[5]) and controlled using mass-spectrometric method.[2] In the majority of papers, the object of the study is vapor of distilled water of normally unknown composition. At the same time, the presence of qualitatively the same effect indicates that interaction with water vapor, rather than admixtures, is recorded. It can be thought to be proved[35] that the initial product is not the dimer $(H_2O)_2$ or the complex $(H_2O)_n$ (the recent theoretical publications[40] showed that the first singlet state S_1 in them is dissociative, as well as in the monomer, and the peak of the absorption band at the transition $S_0 \rightarrow S_1$ shifts toward shorter waves). It is also proved[33] that the observed broadband fluorescence does not relate to the OH radical.

An important aspect is also the procedure of filling the measurement cells with water vapor. This factor is mentioned in Ref. 2, where the long exposure was likely needed to saturate adsorption on walls. Large-volume cells must be less critical to this factor because of the large ratio of the volume to the wall area. On the other hand, reproducibility of measurements for water vapor in a 110-m cell[19] significantly depends on the filling rate and mode.[41]

Absorption spectra

The spectral dependences of the absorption coefficients of water vapor and liquid water in the near-UV spectral region are depicted in Fig. 16. It is worthy to note the following facts.

1. The statement[20] that the spectral dependence of the absorption coefficients is the same for liquid water and water vapor (equation (1) being, in fact, the empiric Urbach rule for the edge of an absorption band in ion crystals and some semiconductors) seems to be not valid at least because the positions of the $S_0 \rightarrow S_1$ absorption bands of vapor and liquid water do not coincide (the corresponding energy level diagrams are given in Ref. 22). It is also hard to surmise that the experimental sensitivity in Ref. 20 was sufficient for recording that weak absorption. Besides, there is a discrepancy with the results of Ref. 16 (and Ref. 17) as regards the shape of the spectral dependence.

2. In the region of 266–271 nm, the absorption coefficients determined by spectrophotometric [$3 \cdot 10^{-6}$ (Ref. 16), $2.7 \cdot 10^{-6}$ (Ref. 17), $(1.7–1.8) \cdot 10^{-6}$ (Ref. 19), $0.8 \cdot 10^{-6}$ cm^{-1}·Torr^{-1} (Ref. 18)] and photo-acoustic [$1.2 \cdot 10^{-7}$ (Ref. 25) and $1.3 \cdot 10^{-7}$ cm$^{-1} \cdot$ Torr^{-1} (Ref. 24)] methods differ widely. Since this difference is larger for the larger number of reflections underwent by radiation in a multipass cell, it is natural to suppose that it is connected with the presence of water molecules adsorbed by surfaces of mirrors and windows in the cell.

The effect of adsorption can be assessed based on data from Ref. 42, in which it is shown that water vapor in an ozonometer cell leads to extra attenuation of the UV radiation. This attenuation correlates with the quality of window processing, the difference in which becomes noticeable only when using the method of electron microscopy. The recalculation of the presented data shows that at the water vapor pressure of 7.5 Torr the transmittance of one surface is from 0.9989 to 0.9954. In Ref. 16, the radiation passing 48 times through the cell undergoes 47 reflections and thus passes 96 times through the "film" ($2 \cdot 47 + 2$ windows). Thus, the cell transmittance may drop from 0.8997 to 0.6455 due to this effect. The experimentally measured transmittance of the cell with water vapor at the wavelength of 270 nm was 0.732 (Ref. 16), wherefrom the absorption coefficient was found to be $3 \cdot 10^{-6}$ cm^{-1}·Torr^{-1}. As is seen, the allowance for the decrease of the cell transmittance due to adsorbed molecules can reduce the absorption coefficient down to zero, however this likely produces no effect on the spectral behavior of the absorption coefficient.

Significant overestimation of the absorption coefficient in Refs. 16 and 17 was also mentioned in Ref. 14, in which, to compare the experimentally measured[13] and the calculated atmospheric transmittance in the region of 310–340 nm, the values of the absorption coefficients from Refs. 16 and 17 were decreased by 20 times.

3. The absorption coefficient[16,17] increases sharply with the decreasing wavelengths and reaches its maximum at the edge of a region (270 and 265 nm, respectively). Therefore, it is too problematic to say about the existence of an absorption band positioned near 270 nm.

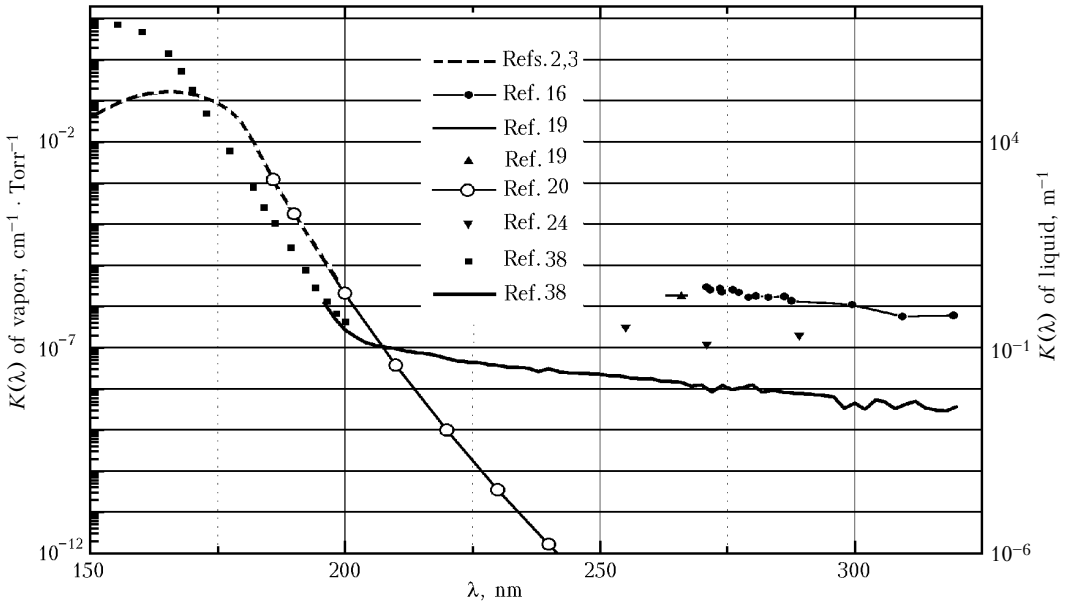

Fig. 16. Spectral dependences of the absorption coefficient of liquid water (according to data from Ref. 38) and water vapor.

4. Now there is no explanation to different spectral behavior of the absorption coefficients reported in Refs. 16, 17, and 25. The cause is likely that the spectrophotometric measurements determine the total extinction, whereas the photo-acoustic measurements determine only the part connected with nonradiative relaxation of excitation. In this connection, it is interesting to consider the behavior of photo-acoustic signal in a mixture of water vapor with argon (see Fig. 4), corresponding to the absorption coefficient roughly doubled as compared to the mixture with nitrogen. The comparison of this peculiarity with the absence of quenching of water vapor fluorescence by argon[33] can point also to the fact that signals recorded in Refs. 16, 17, 25, and 33 are connected with different relaxation channels.

Fluorescence

The quantitative characteristics of fluorescence are tabulated in Table 3. They, in general, agree with each other, especially, in relation to the quenching cross sections that are determined most reliably. The time dependences of fluorescence, in particular, the presence of long-lived component in the central part of the spectrum, agree as well.

The fluorescence in the intervals of 265–275 nm and 300–360 nm depends differently on the power of the exciting radiation and the pressure of water vapor: the dependence is nonlinear in the first interval[29,48] and linear in the second interval.[31,36] This difference is possibly connected with several fluorescing objects caused by the complex character of the photochemical processes involved.

The quantum yield of the integral fluorescence at excitation in the region of 266–270 nm as determined from comparison of fluorescence cross sections with the absorption measured by the photo-acoustic method is 0.15–0.75.

Table 3. Water vapor fluorescence parameters

Excitation wavelength, nm	Fluorescence cross section, 10^{-24} cm^2	Absorption coefficient, $10^{-7} cm^{-1} \cdot Torr^{-1}$	Quenching cross section, 10^{-15} cm^2
212.8	2	0.7	by water vapor – 270
248.5	1.1	0.4	by argon – low nitrogen – 10^{-2} air – 0.5 oxygen – 10
266	0.56 at 24°C 6.9 at 72°C	0.2	by water vapor – 1.5
270	2.5	0.9	–
308	0.1	0.04	–
337	–	0	–

A particular attention should be paid to the behavior of the fluorescence cross section at excitation by the KrF* laser (248.5 nm). The low (as compared to the case of 270 nm) value of fluorescence[26] is, in fact, the only (except for the "extreme" behavior of the absorption coefficients in Ref. 25) argument in favor of the existence of the so-called 270-nm band. On the other hand, the dependence of the Raman scattering cross section on the exciting wavelength (Table 4) could serve an indirect confirmation of the existence of this band[43,44]: the increased value of the cross section at 270 nm may be connected with the resonance character of the effect of this band. At the same time, the reliability of the obtained Raman scattering cross sections is low, as a rule (see the review in Ref. 44).

Table 4. Relative Raman scattering cross sections of water vapor

Observation angle, deg	Excitation wavelength, nm		
	248	266	337
90	0.5 – 1.4	2.9	1.6 – 4.6
180	0.5 – 8	–	–

Possible mechanisms

At present there are no explanations of the whole set of the results obtained. In Ref. 45, an attempt was undertaken to explain the experiments with the KrF* laser (wavelength of 248 nm) by dissociation of water molecules into H + OH and H_2 + O with the following recombination causing the observed glowing. A principle point in such an approach is that the energy of a laser quantum (4.99 eV) is close to the potentials of dissociation (5.12 and 5.0 eV) through the above channels. However, this approach can hardly be automatically extended to longer wavelengths; remind that the fluorescence at excitation by the radiation at 270 nm (the quantum energy of 4.59 eV) is twice as high as that in the case of 248.5 nm and the radiation at 308 nm (3.95 eV) also markedly excites the fluorescence. The dissociative mechanism can likely be invoked to analysis of the results of interaction of water molecules with the radiation having the wavelength of 212.8 nm. At the same time, the possible contribution of the dissociative mechanism is indicated by the results of Ref. 24 on observation of the ionization signals, because the energy threshold of dissociation is lower than that of the ionization.

It seems to be quite probable that the fluorescence excited by the radiation at the wavelength of 248.5 nm and higher occurs in the system of ground-state rotational-vibrational transitions interacting with the first excited electronic states $^1B_1$ and $^3B_1$, although it is traditionally accepted that the rotational-vibrational absorption spectrum of H_2O in the UV region is rather weak. It is usually assumed that the strongest bands can be connected only with high overtones of the stretching vibrations. The centrifugal effect – the strongest intramolecular effect in the H_2O molecule – is usually ignored, as well as possible interaction with excited electronic states. It is known[46,47] that the centrifugal distortion leads to appearance of lines of very weak bands in the spectrum; thus, transitions to such highly excited bending state as (0 10 0) are observed. The interaction of high rotational-vibrational levels of the ground electronic state with the excited electronic states in the water molecule in the presence of strong centrifugal distortion may lead to rather strong mixing of wave functions. This mixing, in its turn, leads to intensity "borrowing" by weak transitions and to appearance of relatively intense H_2O absorption band in the near-UV region.

The spectral behavior of the water vapor absorption coefficient, similar to the wing of the electronic band of liquid water (see Fig. 16), and the temperature dependence of fluorescence agree with this hypothesis.

Conclusions

1. All experimental results clearly demonstrate the presence of interaction between the UV radiation and water vapor. However, there is a serious quantitative discrepancy between the results: the opposed spectral behavior and the 30 times difference in the value of the measured absorption coefficient.

2. The available experimental data and model representations are insufficient for the exhaustive explanation of the nature of the observed absorption and the following fluorescence. In particular, they cannot confirm or refute the hypothesis[26] about the earlier unknown vibrational-electronic band.

3. It is worth conducting additional experiments of a combined study, using different methods in a single setup, for example, recording simultaneously the fluorescent, photo-acoustic, and ionization signals for every laser pulse in a wide range of intensities of the exciting radiation. Upon such measurements are conducted for different pressures and temperatures, it becomes possible to separate the channels of radiative and nonradiative relaxation of the excitation. It is also necessary to measure the fluorescence spectrum with high resolution, what opens the possibility of revealing the structure of the lower states of the transition. Direct measurements of the water vapor absorption spectrum in the region of 200–270 nm are of undoubted interest. In all measurements, the composition of the used water samples should be necessarily controlled.

4. As to theoretical studies, it is worth calculating the energy levels and wave functions of high rotational-vibrational states of H_2O vapor with the allowance for centrifugal effect and the interaction with the first excited electronic states. To determine the model and to choose the centrifugal distortion constants, the results of highly accurate *ab initio* calculations like that in Ref. 15 can be used.

Acknowledgments

This work was partly supported by Russian Foundation for Basic Research Grants No. 00–15–98589 and No. 01–05–65338.

References

1. A.D. Bykov, Yu.S. Makushkin, and O.N. Ulenikov, *Rotational-Vibrational Spectroscopy of Water Vapor* (Nauka, Novosibirsk, 1989), 296 pp.; A.D. Bykov, L.N. Sinitsa, and V.I. Starikov, *Experimental and Theoretical Methods in Molecular Spectroscopy of Water Vapor* (SB RAS Publishing House, Novosibirsk, 1999), 376 pp.

2. K. Watabene and M. Zelikoff, J. Opt. Soc. Am. **43**, No. 9, 753–755 (1953).

3. B.A. Thompson, P. Harchek, and R.R. Reeves, Jr., J. Geophys. Res. **68**, No. 24, 6431–6436 (1963).

4. P.G. Wilkinson and H.L. Johnston, J. Chem. Phys. **18**, No. 2, 190–193 (1950).
5. H.T. Wang, W.S. Felps, and S.P. McGlynn, Chem. Phys. Lett. **67**, No. 6, 2614–2628 (1977).
6. A.M. Pravilov, *Photoprocesses in Molecular Gases* (Energoizdat, Moscow, 1992), 350 pp.
7. Yu.G. Vainer, L.P. Malyavkin, P.M. Nazarov, Sh.D. Fridman, and V.D. Titov, Meteorol. Gidrol., No. 12, 39–47 (1980).
8. M.A. Buldakov, I.I. Ippolitov, V.M. Klimkin, I.I. Matrosov, and V.M. Mitchenkov, in: *Abstracts of Reports at the VIII All-Union Symposium on Laser and Acoustic Sensing of the Atmosphere* (IAO SB AS USSR, Tomsk, 1984), Part 1, pp. 324–326; pp. 338–340.
9. J.J. Hopfield, Phys. Rev. **77**, No. 4, 560–561 (1950).
10. A.N. Krasovskii, A.M. Lyudchik, L.Ch. Neverovich, L.N. Turyshev, V.A. Vartanyan, S.V. Dolgii, and Yu.A. Klimov, Atmos. Oceanic Opt. **5**, No. 5, 329–331 (1992).
11. D.L. Rosen and J.B. Gillespie, Appl. Opt. **28**, No. 19, 4260–4261 (1989).
12. E.M. Patterson and J.B. Gillespie, Appl. Opt. **28**, No. 3, 425–429 (1989).
13. K.A. Burlakov-Vasil'ev and I.E. Vasil'eva, Izv. Ros. Akad. Nauk, Fiz. Atmos. Okeana **28**, No. 12, 1170–1175 (1992).
14. N.F. Borisova and V.M. Osipov, Atmos. Oceanic Opt. **11**, No. 5, 382–386 (1998).
15. H. Partridge and D. Schwenke, J. Chem. Phys. **106**, No. 11, 4618–4639 (1997).
16. S.F. Luk'yanenko, T.I. Novakovskaya, and I.N. Potapkin, Atm. Opt. **2**, No. 7, 579–582 (1989).
17. S.F. Luk'yanenko, T.I. Novakovskaya, and I.N. Potapkin, Atm. Opt. **3**, No. 11, 1080–1082 (1990).
18. S.E. Karmazin, V.M. Klimkin, S.F. Luk'yanenko, M.M. Makogon, I.N. Potapkin, I.S. Tyryshkin, V.N. Fedorishchev, and A.L. Tsvetkov, in: *Abstracts of Reports at the IX All-Union Symposium on High-Resolution Molecular Spectroscopy* (IAO SB AS USSR, Tomsk, 1989), p. 50.
19. Yu.N. Ponomarev and I.S. Tyryshkin, Atmos. Oceanic Opt. **6**, No. 4, 224–228 (1993).
20. N.P. Romanov and V.S. Shuklin, in : *Abstracts of Reports at the VIII All-Union Symposium on Laser and Acoustic Sensing of the Atmosphere* (IAO SB AS USSR, Tomsk, 1984), Part 1, pp. 215–217.
21. R.E. Verral and W.A. Senior, J. Chem. Phys. **50**, No. 6, 2746–2750 (1969).
22. F. Williams, S.P. Varma, and S. Hillenius, J. Chem. Phys. **64**, No. 4, 1549–1554 (1976).
23. A.P. Zuev and A.Yu. Starikovskii, Zh. Prikl. Spektrosk. **52**, No. 3, 455–465 (1990).
24. V.A. Kapitanov, B.A. Tikhomirov, V.O. Troitskii, and I.S. Tyryshkin, Proc. SPIE **3090**, 204–207 (1997).
25. B.A. Tikhomirov, V.O. Troitskii, V.A. Kapitanov, G.S. Evtushenko, and Yu.N. Ponomarev, Acta Phys. Sin. **47**, No. 3, 190–195 (1998).
26. V.M. Klimkin and V.N. Fedorishchev, Atm. Opt. **2**, No. 2, 174–175 (1989).
27. V.M. Klimkin, S.F. Luk'yanenko, I.N. Potapkin, and V.N. Fedorishchev, Atm. Opt. **2**, No. 3, 258–259 (1989).
28. M.A. Buldakov, I.I. Ippolitov, V.M. Klimkin, I.I. Matrosov, and V.M. Mitchenkov, Zh. Prikl. Spektrosk. **46**, No. 4, 554–558 (1987).
29. V.M. Mitchenkov, I.I. Ippolitov, and V.M. Klimkin, Khimiya Vysokikh Energii **22**, No. 1, 58–61 (1988).
30. I.I. Ippolitov, V.M. Klimkin, V.M. Mitchenkov, V.G. Sokovikov, and V.D. Shelevoi, in: *Spectroscopic Methods for Atmospheric Sensing* (Nauka, Novosibirsk, 1985), pp. 107–113.
31. V.M. Klimkin and V.N. Fedorishchev, Opt. Atm. **1**, No. 7, 72–76 (1988).
32. M.N.R. Ashfold, J.M. Bayley, and R.N. Dixon, J. Chem. Phys. **79**, No. 8, 4080–4082 (1983) and Chem. Phys. **84**, No. 1, 35–50 (1984); C.G. Atkins, R.G. Briggs, J.B. Halpern, and G. Hancock, Chem. Phys. Lett. **152**, No. 1, 81–86 (1988) and J. Chem. Soc. Faraday Trans. Part 2. **85**, No. 12, 1987–1997 (1989); S. Niloufar, R. Joelle, L.J. Louis, and R. Francois, Chem. Phys. Lett. **152**, No. 1, 75–80 (1988); K. Mikulesky, K.-H. Gericke, and F.J. Comes, Ber. Bunsenges. Phys. Chem. **95**, No. 8, 927–929 (1991).
33. V.M. Klimkin and V.N. Fedorishchev, Opt. Atm. **1**, No. 8, 26–30 (1988).
34. E.S. Kuznetsova and M.V. Podkolodenko, Zh. Prikl. Spektrosk. **8**, No. 3, 505–506 (1968).
35. S.E. Karmazin, A.N. Kuryak, M.M. Makogon, and A.L. Tsvetkov, Atmos. Oceanic Opt. **8**, No. 11, 937–939 (1995).
36. A.N. Kuryak and M.M. Makogon, in*: Abstracts of Reports at the VIII International Symposium on Atmospheric and Ocean Optics. Atmospheric Physics,* Irkutsk (2001), pp. 90–91; Atmos. Oceanic Opt. **14**, No. 10 (2001) in press.
37. R.A.J. Litjens, T.I. Quickenden, and C.G. Freeman, Appl. Opt. **38**, No. 7, 1216–1223 (1999).
38. T.I. Quickenden and J.A. Irvin, J. Chem. Phys. **72**, No. 8, 4416–4428 (1980).
39. N.P. Grudinkina, Opt. Spektrosk. **1**, No. 5, 658–662 (1956).
40. N.A. Zvereva and I.I. Ippolitov, Izv. Vyssh. Uchebn. Zaved., Ser. Fiz. **42**, No. 5, 8–12 (1999); N.A. Zvereva, Izv. Vyssh. Uchebn. Zaved., Ser. Fiz. **42**, No. 9, 87–91 (1999); N.A. Zvereva, Opt. Spektrosk. **91**, No. 1, 1–5 (2001).
41. I.S. Tyryshkin, private communication.
42. C.P. Meyer, C.M. Elsworth, and I.E. Galbally, Rev. Sci. Instrum. **62**, No. 1, 223–228 (1991).
43. M.A. Buldakov, I.I. Ippolitov, V.M. Klimkin, I.I. Matrosov, and V.M. Mitchenkov, Opt. Spektrosk. **66**, No. 5, 1043–1045 (1989).
44. I.I. Kondilenko, P.A. Korotkov, V.A. Klimenko, and O.P. Dem'yanenko, Opt. Spektrosk. **43**, No. 4, 645–649 (1977).
45. I.I. Ippolitov, "*Spectroscopic Methods and Means for Diagnostics of Natural and Technogenic Media*," Doct. Phys.-Math. Sci. Dissert., Tomsk (1994), 436 pp.
46. A.D. Bykov, O.V. Naumenko, and L.N. Sinitsa, Atm. Opt. **3**, No. 10, 1014–1016 (1990).
47. J.-M. Flaud, C. Camy-Peyret, A. Bykov, O. Naumenko, T. Petrova, A. Scherbakov, and L. Sinitsa, J. Mol. Spectrosc. **185**, No. 1, 211–221 (1997).
48. M.A. Buldakov, I.I. Ippolitov, V.M. Klimkin, I.I. Matrosov, and V.M. Mitchenkov, in: *Abstracts of Reports at the XII All-Union Conference on Coherent and Nonlinear Optics* (MSU Publishing House, Moscow, 1985), Part 2, pp. 121–122.